DOI: 10.1002/ejic.200900373

Cytotoxic Rhodium(III) Polypyridyl Complexes Containing the Tris(pyrazolyl)methane Coligand: Synthesis, DNA Binding Properties and Structure–Activity Relationships

Ruth Bieda,[a] Ingo Ott,[b] Ronald Gust,[c] and William S. Sheldrick*[a]

Keywords: Rhodium / Polypyridyl ligands / Tris(pyrazolyl)methane / Antitumor agents / DNA cleavage

The Rh^{III} complexes of the type $[RhCl(pp)(tpm)]^{2+}$ [pp = bpy, bpm, phen, tap, dpq, dppz] **4**–**9** have been prepared by stepwise treatment of $RhCl_3 \cdot 3H_2O$ or *mer*,*cis*-$[RhCl_3(DMSO\text{-}\kappa S)_2(DMSO\text{-}\kappa O)]$ with the appropriate polypyridyl ligand (pp) followed by the tripodal ligand tris(pyrazolyl)methane (tpm). Intermediates of the type $[RhCl_3(CH_3OH)(pp)]$ **1**–**3** with pp = bpy, phen, dpq were also characterized but exhibit either low (**3**) or no (**1**, **2**) cytotoxicity. X-ray structural analyses of $[RhCl(bpy)(tpm)][PF_6]_2$ **4** and $[RhCl(phen)(tpm)][PF_6]_2$ **6** were performed, and the interaction of complexes **4**–**9** with DNA was investigated by CD and UV/Vis spectroscopy and by gel electrophoresis. CD and viscosity studies confirm strong intercalation of dppz complex **9** into DNA. Complexes **8** and particularly **9** (IC_{50} = 0.43, 0.37 μM) are potent cytotoxic agents towards the human cancer cell lines MCF-7 and HT-29, whereas respectively little (complex **6**) or no activity (complexes **4**, **5**, **7**) is observed for the other members of the series. Our findings indicate that the cytotoxicity is dependent on the hydrophobicity of both the polypyridyl and the facial coligand in these and other half-sandwich Rh^{III} complexes. Irradiation of bpy compound **4** in the presence of plasmid pBR322 for 30 min at 311 nm at a molar ratio of r = 0.1 leads to total conversion of the supercoiled form into the nicked version. Although dppz complex **9** also functions as a photonuclease under these conditions, the degree of cleavage is much lower.

Introduction

Transition-metal polypyridyl (pp) complexes that can target specific base sequences in DNA have received considerable attention as potential diagnostic agents.[1–3] Whereas octahedral ruthenium(II) and rhodium(III) compounds containing 2,2′-bipyridine (bpy) or 1,10-phenanthroline (phen) ligands have been shown to be groove binders or possible partial intercalators,[1,4] strong intercalative binding has often been established when a larger polypyridyl ligand is present. For instance, head-on intercalation has been confirmed for the 9,10-diaminophenanthroline (phi) ligand of Δ-α-$[Rh\{(R,R)\text{-}Me_2trien\}(phi)]^{3+}$ [(*R*,*R*)-Me_2trien = (2*R*,9*R*)-diamino-4,7-diazadecane] in the crystal structure of its adduct with a model hexanucleotide.[5] The alternative side-on intercalation mode was established for half-sandwich complexes of the type $[(\eta^5\text{-}C_5Me_5)Ir(dppz)(L)][CF_3SO_3]_2$ and $[(\eta^6\text{-}C_6Me_6)Ru(dppz)(L)][CF_3SO_3]_2$ (dppz = dipyrido[2,3-*a*:2′,3′-*c*]phenazine) with monodentate κ*S*-coordinated methionine-containing amino acids or peptides L.[6,7]

Whereas octahedral metallointercalators containing two or three polypyridyl ligands have not shown particular promise as anticancer agents,[3] both $[(\eta^5\text{-}C_5Me_5)IrCl(dppz)][CF_3SO_3]$ and $[(\eta^5\text{-}C_5Me_5)RuCl(dppz)][CF_3SO_3]$ exhibit significant in vitro cytotoxicity towards human MCF-7 (breast cancer) and HT-29 (colon cancer) cell lines.[8] In contrast, the phototoxic agent $[RhCl_2(dppz)(phen)]Cl$ exhibits no appreciable degree of cell toxicity towards human tumor cells in the absence of UV irradiation.[9] Despite the great current interest in the development of nonplatinum metal complexes for tumor therapy,[10–12] studies on the cytotoxicity of group 9 transition-metal complexes have been otherwise rather limited.[13–15] However, very recent work on rhodium(III) complexes has produced some highly promising results, in particular for compounds containing a single large polypyridyl ligand. For instance, the meridional trichloro complexes *mer*-$[RhCl_3(DMSO)(pp)]$ (pp = bpy, phen, dpq, dppz, dppn; dpq = dipyrido[3,2-*d*:2′,3′-*f*]quinoxaline; dppn = benzo[*i*]dipyrido[3,2-*a*:2′,3′-*c*]phenazine) are extremely potent and exhibit IC_{50} values in the range 0.051–0.095 μM towards the MCF-7 and HT-29 cell lines for the larger polypyridyl ligands pp = dpq, dppz, dppn.[16–18] Systematic studies on the half-sandwich complexes $[(\eta^5$-

[a] Lehrstuhl für Analytische Chemie, Ruhr-Universität Bochum, Universitätsstraße 150, 44780 Bochum, Germany
Fax: +49-234-3214420
E-mail: william.sheldrick@rub.de
[b] Institut für Pharmazeutische Chemie, Technische Universität Braunschweig,
Beethovenstraße 55, 38106 Braunschweig, Germany
E-mail: Ingo.Ott@tu-bs.de
[c] Institut für Pharmazie, Freie Universität Berlin,
Königin-Luise-Straße 2+4, 14195 Berlin, Germany
Supporting information for this article is available on the WWW under http://dx.doi.org/10.1002/ejic.200900373.

C_5Me_5)RhCl(pp)][CF_3SO_3] (pp = bpy, phen, dpq, dppz, dppn) have demonstrated that the in vitro cytotoxicity of this different type of rhodium(III) complex also increases with increasing polypyridyl ligand size.[19] Significant levels of cell cytotoxicity have also been reported for *mer*-[$RhCl_3$(tpy)] (tpy = 2,2′:6,2′′-terpyridine),[20] *mer,cis*-[$RhCl_3(DMSO)_2(NH_3)$][21] and *fac*-[$RhCl_3$([9]aneNS_2)] ([9]aneNS_2 = 1-aza-4,7-dithiacyclononane)[22] towards various human cancer cell lines.

Changing the six-electron facial coligand in half-sandwich complexes of the general type [MCl(coligand)(pp)]$^{n+}$ can alter the overall cation charge and will affect both the lability of the *trans*-sited M–Cl bond and the steric demand and hydrophobicity of the compound. As these factors can influence both the kinetics and the possible nature of the interaction with DNA or other potential target molecules, it is reasonable to postulate that the biological activity of such complexes will also be affected by the choice of coligand. This line of reasoning led us recently to study the properties of complexes of the type *fac*-[RhCl(pp)([9]aneS_3)]$^{2+}$ ([9]aneS_3 = 1,4,7-trithiacyclononane).[23] These contain the trithia macrocycle [9]aneS_3 whose ability to coordinate rhodium(III) atoms in a facial manner had been previously documented.[24] Whereas the complexes with the larger polypyridyl ligands pp = phen, dpq, dppz are significantly less active than their (η^5-C_5Me_5)Rh^{III} counterparts, this order is surprisingly reversed for the 2,2′-bipyridine complex. This exhibits IC_{50} values of 12.8 (0.2) and 4.4 (0.1) μM (standard deviation are given here and throughout the manuscript in brackets) towards MCF-7 and HT-29 cells, in contrast to [(η^5-C_5Me_5)RhCl(bpy)]$^+$, which is effectively inactive (IC_{50} > 100 μM).[19] These changes in the structure–activity relationships and the observed nuclease activity of *fac*-[RhCl(dpq)([9]aneS_3)]$^{2+}$ prompted us to study the effect of introducing the harder N-donor set of the tripodal six-electron donor ligand tris(pyrazolyl)methane (tpm), for which an increased steric demand can be expected (Scheme 1).

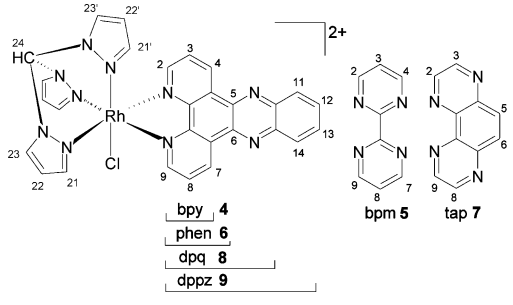

Scheme 1. Structures of the cations of the tris(pyrazolyl)methane complexes **4**–**9**.

Whereas {(tpm)Rh^I} complexes are known,[25,26] to the best of our knowledge only rhodium(III) compounds of the type [RhCl(pp)(tpm*)][PF_6]$_2$ (pp = bpy, phen), [$RhCl_2$(py)(tpm*)][PF_6] and [RhCl(py)$_2$(tpm*)][PF_6]$_2$ with the tris(3,5-dimethylpyrazolyl)methane ligand (tpm*) have been previously reported.[27] The authors of this latter study (J. A. Thomas et al.) were unsuccessful in obtaining {(tpm)-Rh^{III}} complexes and observed only the formation of "yellow intractable solids" on reacting $RhCl_3$·3H_2O with tpm.

We now report the synthesis, DNA binding properties and biological activity of the complexes *fac*-[RhCl(pp)(tpm)]$^{2+}$ **4**–**9** (pp = bpy, bpm, tap, phen, dpq, dppz; bpm = 2,2′-bipyrimidine, tap = pyrazino[2,3-*f*]quinoxaline), which were obtained by treating intermediates of the type *fac*/*mer*-[$RhCl_3$(pp)(CH_3OH)] with tris(pyrazolyl)-methane. To allow a comparison with the highly potent DMSO complexes[16] of the type *mer*-[$RhCl_3$(DMSO)(pp)], the cytotoxicity of the selected intermediates **1**–**3** (Scheme 2) was also studied.

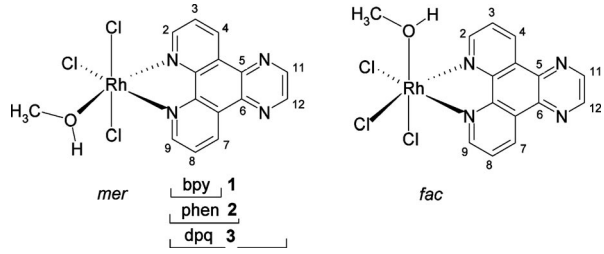

Scheme 2. *fac*- and *mer*-Isomers of the complexes **1** –**3**.

Results and Discussion

Neutral Intermediate Products 1–3

Reaction of $RhCl_3$·3H_2O and 2,2′-bipyridine in methanol at 78 °C led to rapid precipitation of an orange solid that contained a mixture of the *fac* and *mer* isomers of [$RhCl_3$(bpy)(CH_3OH)] with the former isomer clearly predominating in methanol solution on the basis of ^{1}H NMR spectroscopic data.[23] However, on leaving the mother liquor to stand, the latter isomer *mer*-[$RhCl_3$(bpy)(CH_3OH)·CH_3OH (**1**) slowly crystallized from the remaining solution in the form of red prismatic crystals and its coordination geometry was confirmed by X-ray diffraction.[23] The trichlorido intermediates *fac*/*mer*-[$RhCl_3$(CH_3OH)(phen)] (**2**) and *mer*-[$RhCl_3$(CH_3OH)-(dpq)] (**3**) (Scheme 2) were isolated in a similar manner with the appropriate polypyridyl ligand.

^{1}H NMR studies demonstrate that the *fac* isomers of **1**–**3** predominate in the *fac*/*mer* mixtures present in polar solvents. IC_{50} values for **1**–**3** are listed in Table 1 and show that complexes **1** and **2** are inactive (IC_{50} > 100 μM) towards MCF-7 and HT-29 cells. In contrast, the *mer* isomers of the analogous DMSO compounds [$RhCl_3$(DMSO)(pp)] (pp = bpy, phen, dpq) **1a**–**3a** are highly potent towards MCF-7 and HT-29 cell lines and exhibit IC_{50} values of 4.0 and 1.9 μM for pp = bpy, 0.40 and 0.19 μM for pp = phen and 0.079 and 0.069 μM for pp = dpq.[16] Although equilibrium mixtures of *fac* and *mer* isomers of the DMSO compounds are significantly less cytotoxic[18] than the *mer* isomers alone, they are still quite active (Table 1). A dramatic reduction in the level of cellular uptake in comparison to the DMSO complexes may possibly be responsible for the lack of activity of the methanol

Table 1. IC_{50} values (μM) and cellular uptake (ng Rh/mg protein) for the complexes $[RhCl_3(L)(pp)]$ (L = CH_3OH **1**–**3**, DMSO[16,18] **1a**–**3b**) towards the MCF-7 and HT-29 cell lines.

	Isomer	L	pp	Solvent	MCF-7 IC_{50}	HT-29 IC_{50}	MCF-7 uptake[a]	HT-29 uptake[a]
1	*fac*/*mer*	CH_3OH	bpy	H_2O	>100	>100	9.47 (2.15)	4.49 (0.25)
2	*fac*/*mer*	CH_3OH	phen	DMF	>100	>100	2.79 (1.41)	3.15 (0.21)
3	*mer*	CH_3OH	dpq	DMF	29.6 (4.3)	34.0 (5.8)	35.58 (3.80)	2.46 (1.07)
				DMSO	5.3 (0.4)	2.7 (2.1)	n.d.	n.d.
1a	*mer*	DMSO	bpy	DMSO	4.0 (0.5)	1.9 (0.5)	41.6 (0.5)	24.7 (9.2)
2a	*mer*	DMSO	phen	DMSO	0.40 (0.06)	0.19 (0.05)	70.8 (12.2)	49.0 (0.6)
3a	*mer*	DMSO	dpq	DMSO	0.079 (0.012)	0.069 (0.021)	92.1 (1.4)	53.6 (2.0)
1b	*fac*/*mer*	DMSO	bpy	DMSO	5.1 (1.3)	4.0 (1.1)	n.d.	n.d.
2b	*fac*/*mer*	DMSO	phen	DMSO	1.1 (0.2)	0.66 (0.02)	n.d.	n.d.
3b	*fac*/*mer*	DMSO	dpq	DMSO	0.47 (0.03)	0.312 (0.032)	n.d.	n.d.

[a] For 10 μM solutions for **1**–**3** and 1 μM solutions for **1a**–**3a**; n.d. not determined.

complexes. Whereas Rh concentrations of 2.79–9.47 ng Rh/mg protein were measured for MCF-7 and HT-29 cells after incubation periods of 4 h with 10 μM solutions of **1** and **2** (Table 1), much higher levels of 24.7–70.8 ng Rh/mg protein were recorded for *mer*-$[RhCl_3(DMSO)(pp)]$ (pp = bpy, phen) at a ten times lower 1 μM incubation concentration.[16] A similar correlation can be established for the dpq complex **3** in comparison to *mer*-$[RhCl_3(DMSO)(dpq)]$, whose cellular uptake levels are 92.1 and 53.6 ng Rh/mg protein, respectively, for a 1 μM incubation solution.

Although the *mer* isomer of **3** does exhibit moderate cytotoxicity towards the cancer cell lines MCF-7 and HT-29, the recorded IC_{50} values (29.6, 34.0 μM) are much higher than those reported for *mer*-$[RhCl_3(DMSO)(dpq)]$ and an equilibrium mixture of the *fac* and *mer* isomers of $[RhCl_3(DMSO)(dpq)]$ (Table 1).[18] It is interesting to note that a higher cytotoxicity is recorded on dissolving the compound *mer*-$[RhCl_3(CH_3OH)(dpq)]$ **3** in DMSO rather than DMF to afford the stock solution, which is prepared during the first steps of the cytotoxicity assay procedure. A slow CH_3OH/DMSO exchange appears to be responsible for its significantly increased cytotoxicity [IC_{50} = 5.3 (0.4) μM] in DMSO solution towards MCF-7 cells. It can be followed by ^1H NMR kinetic studies for the compounds in DMSO at ambient temperature under roomlight irradiation over a period of a week. Slow exchange reactions were also observed for the complexes $[RhCl_3(CH_3OH)(pp)]$ **1**–**3** and $[RhCl_3(DMSO)(pp)]$ **1a**–**3a** in the polar solvents L = CH_3OH, H_2O. For instance the ratio of coordinated DMSO to free DMSO is 93:7 for complex **2a** after 24 h in methanol at 25 °C.[16] As DMSO/CH_3OH substitution leads to conversion of highly active **2a** to inactive **2** it can be concluded that the initial presence of coordinated DMSO is essential for significant cytotoxicity.

Tris(pyrazolyl)methane Complexes

Synthesis and Structure of Complexes 4 and 6

Two synthesis routes were employed to produce complex cations $[RhCl(pp)(tpm)]^{2+}$ containing polypyridyl ligands (pp = bpy, bpm, phen, tap, dpq and dppz) **4**–**9**. In contrast to the previous report of Thomas et al. on the unsuitability of the $\{(tpm)Rh\}^{3+}$ fragment[27] for generating polypyridyl complexes, these compounds could be obtained in good yields. Here the important factor appears to be that the tpm ligand was added to intermediate polypyridyl complexes in the final step of the synthesis procedure rather than attempting to employ the poorly soluble hypothetical compound $[RhCl_3(tpm)]$ as a starting material. We employed procedures that involve starting from either *mer*,*cis*-$[RhCl_3(DMSO\text{-}\kappa S)_2(DMSO\text{-}\kappa O)]$ or directly from $RhCl_3 \cdot 3H_2O$. The former route was used for the syntheses of the bpy and phen compounds in the early stages of the work and then replaced by the direct strategy involving $RhCl_3 \cdot 3H_2O$ for the remaining complexes **5** and **7**–**9**. Both methods generate $[RhCl(pp)(tpm)]^{2+}$ cations in reasonable to good yields. Following initial treatment with the polypyridyl ligand, tris(pyrazolyl)methane was added to the intermediate products of the type *fac*/*mer*-$[RhCl_3(L)(pp)]$ (L = DMSO, H_2O, CH_3OH) to afford complexes **4**–**9**, which were characterized by ^1H NMR spectroscopy and positive-ion LSIMS and gave satisfactory microanalyses. The complexes **4**–**7** exhibit good and complex **9** reasonable solubility in H_2O or DMSO and were studied in these solvents. Owing to its poor solubility in polar solvents the ^1H NMR spectra of **8** was recorded in CD_2Cl_2. COSY and ROESY 2D NMR spectra in $[D_6]$DMSO and D_2O exhibit correlations of the neighbouring tpm proton signals. There are two sets of resonances for the pyrazole protons in a 1:2 ratio.

Single crystals of $[RhCl(bpy)(tpm)][PF_6]_2$ (**4**) (Figure 1) and $[RhCl(phen)(tpm)][PF_6]_2 \cdot H_2O$ (**6**) (Figure 2) were obtained by slow evaporation from aqueous solutions. One of the two independent hexafluorophosphate counterions in the crystal lattice of **4** is disordered and disorder is also observed for the co-crystallized water molecule in **6**. A comparison of the Rh–Cl bonds indicates a stronger binding of the chloride ligand within the bpy complex with an Rh1–Cl1 value of 2.3087(9) Å in contrast to that of 2.319(3) Å in **6**. In contrast to this finding, the Rh1–Cl1 bond [2.371(1) Å] of the analogous compound $[RhCl(dpq)([9]aneS_3)]Cl_2$[23] is significantly longer than both of these bonds. The precursor *mer*-$[RhCl_3(bpy)(CH_3OH)] \cdot CH_3OH$

(**1**) with no tripodal coligand contains Rh–Cl bonds of 2.356(1) Å, 2.346(1) Å and 2.322(1) Å.[23] It is interesting to note that the phen ligand of **6** is tilted towards the central rhodium coordination plane at an angle of 9.7°, that is almost twice as large as that of 5.1° for the smaller bpy ligand. Differing angles of tilt have also been reported for the pp ligands in $(\eta\text{-}C_5Me_5)Rh^{III}$ complexes.[19]

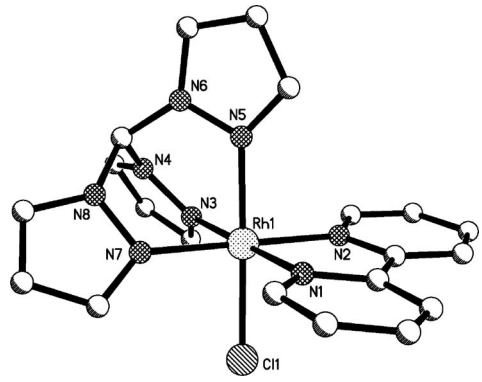

Figure 1. Molecular structure of the dication of [RhCl(bpy)(tpm)][PF_6]$_2$ (**4**).

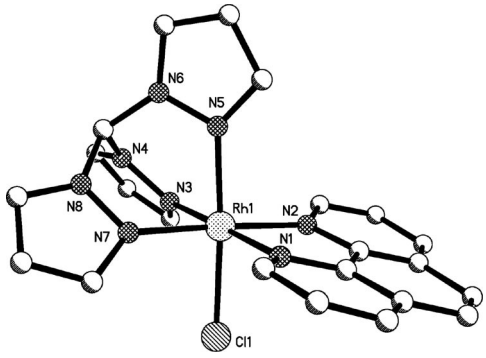

Figure 2. Molecular structure of the dication of [RhCl(phen)(tpm)][PF_6]$_2$·H_2O (**6**).

DNA Binding Studies for 4–9

Changes in the circular dichroism (CD) spectra of DNA in the range of 220–350 nm provide a convenient means of monitoring conformational changes resulting from the addition of transition-metal complexes.[28,29] A negative CD band at 246 nm caused by the helical B conformation and a positive band at 275 nm due to base stacking are characteristic for CT-DNA.[29] No significant changes in this CD spectrum were observed for CT DNA on its mixing with the compound [RhCl(bpy)(tpm)][PF_6]$_2$ (**4**) at a 1:5 molar ratio r {r = [complex]/[DNA] = 0.2 for [DNA] = M(base pairs)} (Figure 3). This was also the case for the complexes **5** and **7** of the nitrogen-rich ligands bpm and tap (Figure S1, Supporting Information). In contrast, the maximum of the base-stacking signal at about 270 nm for CT DNA narrows and is significantly shifted to lower wavelength on mixing the biopolymer with [RhCl(phen)(tpm)][PF_6]$_2$ (**6**). Only minor changes in the negative molar ellipticity value [θ] at 245 nm were observed for CT DNA with **4** and **6**. To assure solubility of the complexes **4**–**9**, 1% DMSO in each case was added to the employed aqueous buffer solutions. For comparison purposes 1% DMSO was also employed for CT DNA alone. As the presence of DMSO causes significant disturbances in the CT DNA spectrum at $\lambda <$ 230 nm, only the 230–400 nm range is depicted.

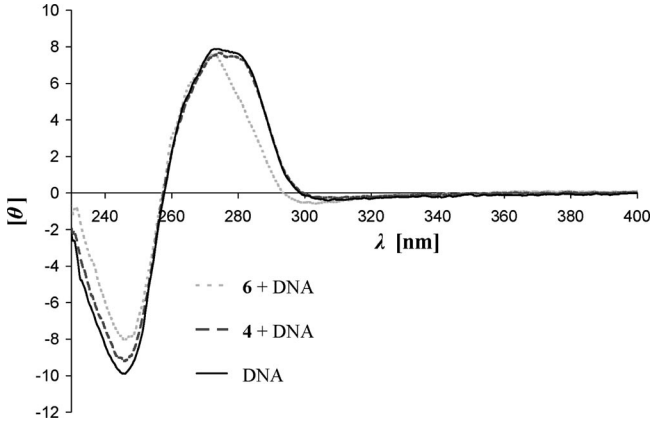

Figure 3. CD spectra of CT DNA alone and with complexes [RhCl(bpy)(tpm)][PF_6]$_2$ (**4**) or [RhCl(phen)(tpm)][PF_6]$_2$ (**6**) {r = [complex]/[DNA] = 0.2 for [DNA] = M(base pairs)} in a 10 mM phosphate buffer (pH = 7.2) after an incubation period of 60 min. Molar ellipticities [θ] are given in the units deg cm^2 dmol^{-1} × 10^{-3}.

The CD band at about 270 nm for the base stacking in DNA is significantly enlarged and shifted to lower wavelength for the compounds [RhCl(dpq)(tpm)]Cl_2 (**8**) and [RhCl(dppz)(tpm)]Cl_2 (**9**) (Figure 4). The CD spectrum of [RhCl(dpq)(tpm)]Cl_2 (**8**) with CT DNA exhibits an 18% increase in positive molar ellipticity [θ] for a maximum at 270 nm. An even greater increase of 48% is observed for the [θ] value of CT DNA in the presence of [RhCl(dppz)(tpm)]Cl_2 (**9**). This increase is accompanied by a hypsochromic shift in λ_{max} to 268 nm, in addition to a negative induced CD signal at 300 nm with a [θ] value of –2.0. These significant changes in the CD absorption of the biopolymer are clearly in accordance with intercalation of the dppz ligand as previously demonstrated for half-sandwich $(\eta^5\text{-}C_5Me_5)Ir^{III}$ and $(\eta^5\text{-}C_5Me_5)Rh^{III}$ complexes.[30,31]

The most convincing evidence for DNA intercalation is provided by viscosity measurements.[32,33] Insertion of large aromatic ligands such as dppz between adjacent nucleobases pairs leads to lengthening and shifting of the double helix and these changes are reflected in an increase in DNA viscosity. Figure 5 illustrates the dependence of the reduced viscosity function $(\eta/\eta_0)^{1/3}$ on the [complex]/[DNA] ratio r for complexes **4** and **9**. As $(\eta/\eta_0)^{1/3}$ is equal to (L/L_0), where L is the length of intercalated DNA and L_0 is the length of DNA alone,[32] a slope of 1 is to be expected for ideal intercalation at lower r values. These values reflect the classical model of intercalation where the helix is lengthened by 3.4 Å per intercalated aromatic moiety. In fact, a wider range of possible helix extensions from 2.0 to 3.7 Å have been indicated by electric dichroism measurements.[34] A slope of 0.9706 was determined for ethidium bromide as a standard strong intercalator using our experimental setup.

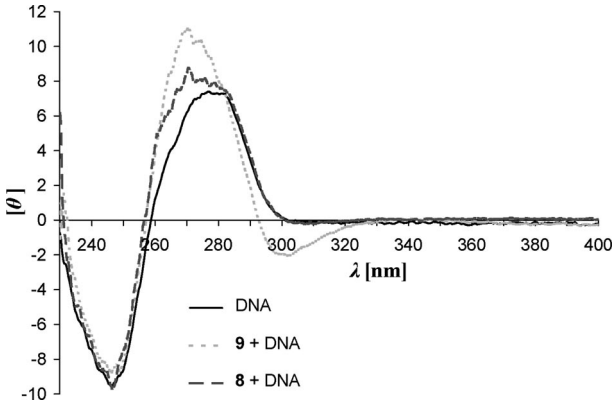

Figure 4. CD spectra of CT DNA alone and with complexes $[RhCl(dpq)(tpm)]Cl_2$ (**8**) or$[RhCl(dppz)(tpm)]Cl_2$ (**9**) {r = [complex]/[DNA] = 0.2 for [DNA] = M(base pairs)} in a 10 mM phosphate buffer (pH = 7.2) after an incubation period of 60 min. Molar ellipticities [θ] are given in the units deg cm^2 dmol$^{-1} \times 10^{-3}$.

The viscosity measurements clearly confirm the intercalative binding mode of $[RhCl(dppz)(tpm)]Cl_2$ **9**. A regression line of $y = 0.8509x + 1$ is obtained for **9** on plotting $(\eta/\eta_0)^{1/3}$ vs. r, in contrast to a slope of only 0.0943 for the bpy compound **4**. Whereas the slope value for **9** is in accordance with strong intercalative binding, the very small increase in DNA length in the presence of complex **4** could possibly be due to covalent or groove binding. A significant degree of intercalation can be ruled out for **4**.

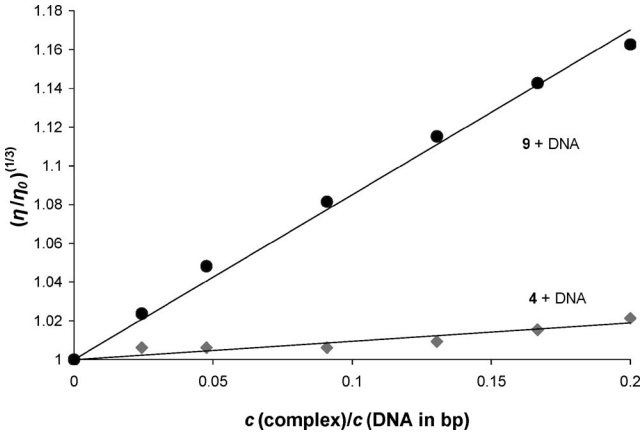

Figure 5. Dependence of $(\eta/\eta_0)^{1/3}$ on r {r = [complex]/[DNA] where [DNA] is given in M (base pairs)} for viscosity measurements of CT DNA with $[RhCl(bpy)(tpm)][PF_6]_2$ (**4**) or $[RhCl(dppz)(tpm)]Cl_2$ (**9**) in a 10 mM phosphate buffer (pH = 7.2). Regression lines are depicted to underline the linear dependence.

Modest thermal denaturation temperature changes of +2, +2, +1, +1, +3, +5 °C were recorded for CT DNA in the presence of complexes **4**, **5**, **6**, **7**, **8**, **9**, respectively, at a molar ratio of r = 0.2 where [DNA] is given in M(base pairs). The larger increase for complex **9** is in accordance with dppz intercalation as established by the viscosity measurements. UV/Vis kinetic studies indicate only minor changes in absorbance in the range of 320–450 nm for complexes **4** and **8** on mixing with DNA. In the case of complex **4**, the absorption maxima at 308 and 318 nm for the compound alone (Figure S2, a, Supporting Information) increase by 3.7 and 2.7%, respectively, within 1 min of mixing with DNA and then remain constant during the following 4 h. The UV/Vis spectrum of $[RhCl(dpq)(tpm)]Cl_2$ (**8**) with DNA at the same molar ratio exhibits a 1% increase within 48 h for the maxima at 330 and 344 nm.

In contrast to $[RhCl(dppz)(tpm)]Cl_2$ (**9**) alone (Figure S2, b), mixing **9** with CT DNA at r = 0.2 leads to large decreases $\Delta A/A$ of –32.5 and –39.7% for the maxima at 364 and 381 nm, respectively, within 1 min (Figure 6). Over the following 12 h, additional decreases of about 3% are observed. The two maxima are shifted by 2 and 1.5 nm, respectively, to higher wavelengths. Small but significant changes were also observed for **9** in the employed phosphate buffer (pH = 7.2) without DNA over a period of 48 h. Decreases of 3.6% and a 0.5 nm shift were recorded for both maxima, suggesting that very slow chloride/phosphate or chloride/water exchange must be taking place.

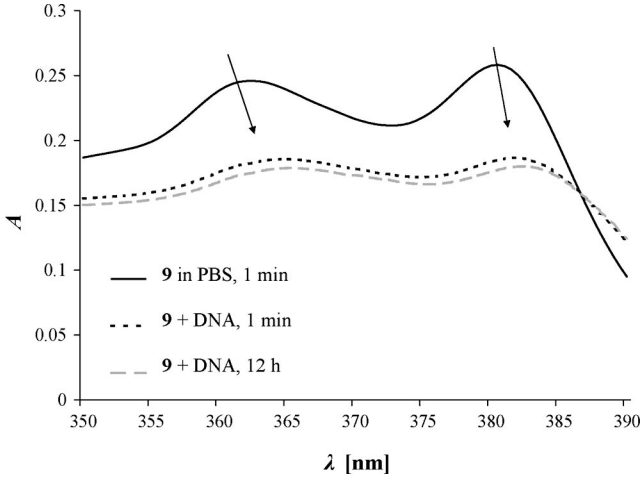

Figure 6. UV/Vis spectrum of the dppz complex **9** in a phosphate buffer (PBS) alone and with CT DNA after 1 min and 12 h, respectively, at r = 0.2 [DNA] with [DNA] = M(base pairs).

DNA Cleavage Properties of 4 and 9

Gel-electrophoresis assays were carried out with plasmid pBR322 (Fermentas) in an agarose gel to analyze possible DNA interaction and light-induced cleavage activity. The first and the last members of the polypyridyl series $[RhCl(bpy)(tpm)][PF_6]_2$ (**4**) and $[RhCl(dppz)(tpm)]Cl_2$ (**9**) were selected as exemplary compounds for the analysis. Initially cleavage properties were studied in the dark and with irradiation under aerobic conditions and at varying concentrations of 2, 5 and 20 μM for the compounds (Figure S3). In each case 20 μM (bp) of double-stranded circular plasmid DNA pBR322 was employed. In the dark, no significant changes were observed for the retardation of the supercoiled plasmid at the various concentrations of compounds **4** and **9**. Following irradiation at 311 nm for 1 h, photonuclease activity could clearly be recognized. At concentrations of 2 and 5 μM of complex **4** almost all the supercoiled DNA was converted into nicked DNA. At a

higher concentration of 20 μM multiple DNA strand breaks appear to be provoked and no significant fragments were detectable by gel electrophoresis. An alternative though unlikely explanation could, however, be that irradiation might lead to stronger DNA binding of compound **4** in comparison to ethidium bromide. Analogous gel electrophoretic observations were made for the compound **9**.

To further characterize the possible nuclease activity of **4** and **9**, both the irradiation time and wavelengths were varied. To begin with, irradiation times of 1 h and 30 min were compared (Figure 7). Lines 1 to 3 of Figure 7 exhibit the results for DNA alone and for complex/DNA mixtures at 2 μM complex and 20 μM DNA (base pairs) concentrations in the dark. No significant cleavage was detected. Irradiation at 311 nm for 30 min (Figure 7, lines 4 and 5) and 1 h, respectively, (Figure 7, lines 7 and 8) led, in contrast, to significant cleavage of the supercoiled plasmid into the nicked version. It is apparent that an irradiation of 30 min is already adequate to accomplish full conversion in the case of complex **4**, which exhibits a pronounced absorption maximum at 320 nm in the presence of DNA. A GeneRuler™1kb DNA ladder (Fermentas) is shown in Figure 7, line 9 as a reference.

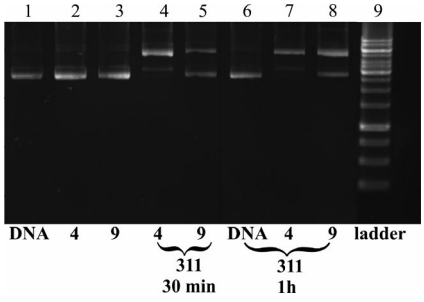

Figure 7. Comparison of DNA cleavage at various irradiation times for compounds **4** (2 μM) and **9** (2 μM) with plasmid pBR322 DNA (20 μM in bp) at 311 nm as determined by a gel-retardation assay. A GeneRuler™1kb DNA ladder (Fermentas) is shown in line 9 as a reference.

In addition to 311 nm, different irradiation wavelengths were chosen to correspond to the small absorption maxima of the compounds in the range 308–382 nm. Whereas the UV/Vis spectrum of compound **4** contains pronounced maxima in the presence of DNA at 311 and 320 nm, that of **9** exhibits two small MLCT maxima at 366 and 382 nm (Figure 6). Figure 8 confirms that 311 nm is the most efficient irradiation wavelength for both compounds.

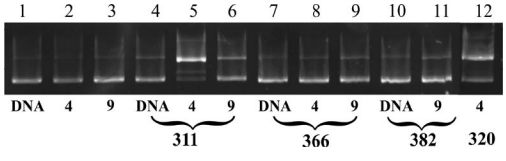

Figure 8. Gel-retardation assay of plasmid pBR322 (20 μM in bp) in the presence of 2 μM concentrations of complexes **4** and **9** after irradiation for 30 min at various wavelengths (311, 366, 382 and 320 nm).

Whereas irradiation of compound **4** and plasmid pBR322 at 320 nm (Figure 8, line 12) also led to the presence of predominantly nicked plasmid, no significant cleavage was recorded following irradiation of **9** plus plasmid at both 366 and 382 nm (Figure 8, lines 9 and 11).

Cytotoxicity of 4–9

In vitro cytotoxicity studies of compounds **4**–**9** were carried out with the human MCF-7 (breast cancer) and HT-29 (colon cancer) cell lines and the resulting IC_{50} values are listed in Table 2. For the compounds **4**, **6**, **8** and **9**, which contain polypyridyl ligands of differing sizes, an increase of the antiproliferative potency with increasing surface area and hydrophobicity of the polypyridyl ligands was to be expected[8] and is indeed observed. It is interesting to also note, that the tpm ligand itself is not cytotoxic toward the MCF-7 and HT-29 cell lines and that the compounds **4** and **6** are less active than bpy and phen alone. This lowering of the cytotoxicity appears to be due to the presence of the $\{(tpm)Rh\}^{3+}$ fragment. In contrast, whereas the monocation $[(\eta^5\text{-}C_5Me_5)RhCl(bpy)]^+$ is also inactive ($IC_{50} >$ 100 μM),[19] relatively high cytotoxicities [12.8 (0.2) MCF-7, 4.4 (0.1) μM HT-29] have been reported for the dication $[RhCl(bpy)([9]aneS_3)]^{2+}$.[23] The cytotoxicity of complex $[(coligand)RhCl(pp)]^{n+}$ increases in dependency on the coligand in the order $\eta^5\text{-}C_5Me_5$, tpm << $[9]aneS_3$ for pp = bpy and in the order tpm, $[9]aneS_3$ << $\eta^5\text{-}C_5Me_5$ for the analogous phen complexes (Table 3). A lack of cytotoxic activity ($IC_{50} > 100$ μM) was also established for the complexes $[RhCl(pp)(tpm)]^{2+}$ **5** and **7**, which contain the nitrogen-rich polypyridyl ligands bpm and tap, respectively. This finding is in striking contrast to the analogous $\{([9]aneS_3)\text{-}Rh\}^{3+}$ complexes for which low IC_{50} values of 1.7 ± 0.5 μM (MCF-7 cells) and 1.9 ± 0.1 μM (HT-29 cells) were recorded for pp = bpm and 11.5 ± 0.6 μM and 7.6 ± 4.8 μM for pp = tap, respectively. Correlating with the increasing aromatic size of the pp ligand in the order phen < dpq < dppz, the cytotoxicity increases dramatically within the $\{(tpm)Rh\}^{3+}$ series **6**, **8** and **9** with the latter complex exhibiting very low

Table 2. IC_{50} (μM) values for the complexes $[RhCl(pp)(tpm)]^{2+}$ **4**–**9** towards MCF-7 and HT-29 cells.

Compound	pp	Counterions	MCF-7 IC_{50}	HT-29 IC_{50}
4	bpy	PF_6	> 100	>100
5	bpm	Cl	> 100	> 100
6	phen	PF_6	51.7(11.9)	83.2 (0.5)
7	tap	Cl	> 100	> 100
8	dpq	Cl	4.0 (0.2)	6.7 (1.0)
9	dppz	Cl	0.43 (0.18)	0.37 (0.06)
tpm			> 100	> 100
bpy[19]			52.7 (7.8)	45.7 (4.6)
phen[19]			3.5 (0.2)	2.7 (0.5)
tap[22]			> 100	> 100
dpq[19]			6.7 (2.0)	7.0 (2.2)
dppz[19]			0.8 (0.6)	1.8 (0.2)
cisplatin[8]			2.0 (0.3)	7.0 (2.0)

Table 3. A comparison of the IC_{50} (μM) values of rhodium(III) polypyridyl complexes $[(coligand)RhCl(pp)]^{n+}$ with different facial coligands towards MCF-7 and HT-29 cells.[a]

pp	Coligand = $[\eta^5\text{-}C_5Me_5]^-$ [19]		Coligand = [9]aneS$_3$ [22]		Coligand = tpm	
	MCF-7	HT-29	MCF-7	HT-29	MCF-7	HT-29
bpy	>100	>100	12.8 (0.2)	4.4 (0.1)	> 100	>100
phen	4.7 (0.1)	8.0 (1.6)	36.3 (6.0)	72.2 (8.0)	51.7(11.9)	83.2 (0.5)
dpq	5.1 (0.2)	8.5 (1.6)	19.1 (0.3)	20.9 (2.8)	4.0 (0.2)	6.7 (1.0)
dppz	1.5 (0.4)	4.3 (0.2)	4.7 (0.5)	7.4 (2.2)	0.43 (0.18)	0.37 (0.06)
bpm	n.d.	n.d.	1.7 (0.5)	1.9 (0.1)	>100	>100
tap	n.d.	n.d.	11.5 (0.6)	7.6 (4.8)	>100	>100

[a] n.d. = not determined.

IC_{50} values of only 0.43 (0.18) and 0.37 (0.06) μM towards the MCF-7 and HT-29 cell lines. Compound **9** is much more potent than cisplatin [2.0 (0.3) for MCF-7 and 7.0 (2.09) μM for HT-29][8] and both $[RhCl(dppz)([9]aneS_3)]^{2+}$ (4.7 and 7.4 μM) and $[(\eta^5\text{-}C_5Me_5)RhCl(dppz)]^+$ (1.5 and 4.3 μM) or dppz itself (0.8 and 1.8 μM).

IC_{50} values for individual complexes with facial coligands are listed in Table 3 and allow the following structure–activity relationships to be established:

1. The influence of the coligand on the increasing cytotoxicity within the series pp = phen, dpq, dppz increases in the order $[\eta^5\text{-}C_5Me_5]^- <$ [9]aneS$_3$ < tpm.

Whereas only a 3.1/1.9 fold increase in cytotoxicity for MCF-7/HT-29 cells is observed for the $(\eta^5\text{-}C_5Me_5)Rh^{III}$ complexes on going from pp = phen to the larger dppz ligand, this factor improves over a factor of 7.7/9.8 for the $\{([9]aneS_3)Rh^{III}\}$ complexes up to 120.2/224.9 for polypyridyl compounds containing the $\{(tpm)Rh^{III}\}$ fragment! The remarkable influence of the tripodal tris(pyrazolyl)methane ligand may well be due to its increased hydrophobicity which should significantly improve the cellular uptake of its polypyridyl compounds. To quantify this effect we determined the cellular uptake of dpq complex **8** by MCF-7 and HT-29 cells using atom absorption spectrometry. Values of 24.0 (0.1) and 11.8 (0.3) ng rhodium/mg protein, which were obtained for the respective cell lines following a 6 h incubation period with **8** at 37 °C/5% CO_2, represent a more than 10-fold increase in comparison to $[(\eta^5\text{-}C_5Me_5)RhCl(dpq)][CF_3SO_3]$.[19] The $(\eta^5\text{-}C_5Me_5)Rh^{III}$ complex affords much lower cellular levels of 11.3 (0.5) and 4.1 (1.7) ng rhodium/mg protein despite its lower overall charge and despite its being present at a 100 μM incubation concentration.

2. The influence of the coligand on the cytotoxicity of the bipyridine complexes increases in the order $[\eta^5\text{-}C_5Me_5]^-$, tpm << [9]aneS$_3$.

Following rapid Cl^-/H_2O exchange,[36] the dication $[(\eta^5\text{-}C_5Me_5)Rh(H_2O)(bpy)]^{2+}$ may be expected to rapidly bind to biomolecules other than the potential target molecules in the cell. A lower reactivity of the tris(pyrazolyl)methane complex could hinder its adequate binding to target molecules. It is possible that an intermediate kinetic stability of the [9]aneS$_3$ complexes may be responsible for their remarkable cytotoxicity in the cases of the smaller polypyridyl ligands pp = bpy, bpm, tap, for which DNA intercalation is not observed.

Conclusions

Tris(pyrazolyl)methane rhodium(III) complexes of the type $[RhCl(pp)(tpm)]^{2+}$ can be prepared by stepwise addition of (a) the chosen polypyridyl ligand followed by (b) the tripodal tpm ligand to either $RhCl_3{\cdot}3H_2O$ or *mer*/*cis*-$[RhCl_3(DMSO)_3]$. $[RhCl(dppz)(tpm)]^{2+}$ (**9**) exhibits intercalative binding into the DNA double helix, as has also recently been reported for the analogous ruthenium(II) dppz complexes $[RuCl(dppz)(tpm)][PF_6]$ and $[Ru(L)(dppz)(tpm)][PF_6]_2$ (L = CH_3CN, pyridine).[35]

The presence of a polypyridyl ligand pp = phen, dpq, dppz leads to cytotoxicity towards MCF-7 and HT-29 cells for rhodium(III) complexes of the general type $[(coligand)RhCl(pp)]^{n+}$ with the facial coligands $[\eta^5\text{-}C_5Me_5]^-$ (n = 1), [9]aneS$_3$ (n = 2) and tpm (n = 2). A particularly striking increase in cytotoxicity of over two orders of magnitude is observed for $\{(tpm)Rh\}^{3+}$ complexes within the series phen < dpq < dppz. The important influence of other ligands on the cytotoxicity of rhodium(III) polypyridyl complexes is also underlined by the lack of activity recorded for the series $[RhCl_3(CH_3OH)(pp)]$ (pp = bpy, phen, dpq) (Table 1), which is in striking contrast to the very low IC_{50} values observed for the analogous DMSO complexes $[RhCl_3(DMSO)(pp)]$.[16] Increases of up to two orders of magnitude in the cellular uptake levels may be responsible for the dramatic increase in activity for the latter series.

Experimental Section

General: UV/Vis spectra were recorded with an Analytik Jena SPECORD 200 spectrometer and CD spectra with a Jasco J-715 instrument in the range 220–400 nm for 1:5 complex/[DNA] mixtures [DNA concentration in M(base pairs)] in a 10 mM phosphate buffer at pH 7.2. To assure the solubility of complexes **4**–**9**, 1% DMSO was added to the aqueous buffer. For comparison purposes 1% DMSO was also employed for the CD spectra of CT DNA alone. LSIMS spectra (LSIMS = liquid secondary ion mass spectrometry) were registered for the mass range m/z = 3000 with a Fisons VG Autospec employing a cesium ion gun (voltage 17 kV) and 3-nitrobenzyl alcohol as the liquid matrix. A Bruker DRX 400 and a Bruker DPX 200 were employed for the registration of ^1H NMR spectra with chemical shifts reported as δ values relative to the signal of the deuterated solvent. Elemental analyses were performed on a Vario EL of Elementar Analysensysteme GmbH. $RhCl_3{\cdot}3H_2O$ and tris(pyrazolyl)methane were obtained from ABCR, 2,2′-bipyrimidine from Alfa Aesar, 1,10-phenanthroline, 2,2′-bipyridine, pyr-

azino[2,3-*f*]quinoxaline (tap), ethidium bromide from Acros Organics, calf thymus DNA (CT DNA) from Sigma Aldrich. The plasmid pBR322 and the gene ruler 1kb DNA ladder were obtained from Fermentas. *mer*/*fac*-[RhCl(bpy)(CH_3OH)] (**1**)[23] and the ligands dpq[37] and dppz[38] were prepared in accordance with literature procedures.

***fac*/*mer*-[$RhCl_3$(phen)(CH_3OH)]·$2H_2O$ (2):** 1,10-Phenanthroline (136.6 mg, 0.76 mmol) was added to $RhCl_3·3H_2O$ (199.9 mg, 0.76 mmol) in CH_2Cl_2/MeOH (1:1; 50 mL) and heated at 64 °C for 3 h. After 30 min an orange precipitate was removed by filtration and the remaining solution was reduced in volume to 5 mL. Compound **2** was precipitated as an orange solid from the solution by addition of diethyl ether and subsequently washed with a small amount of CH_3OH and dried in vacuo. Yield: 67.8% (148.3 mg). $C_{13}H_{12}Cl_3N_2O_1Rh·2H_2O$ (457.51): calcd. C 34.13, H 3.52, N 6.12; found C 34.3, H 3.1, N 6.4. LSIMS: *m*/*z* (%) = 386 (40) $[M – Cl]^+$, 353 (77) $[M – Cl – CH_3OH]^+$, 318 (100) $[M – Cl – HCl – CH_3OH]^+$. ^{1}H NMR (200 MHz, [$D_6$]DMSO, 25 °C): δ = 3.63 (d, 3 H, CH_3, $MeOH_{coor}$), 8.15–8.27 [m, 3 H, phen, *mer*(2H)/*fac*(1H)], 8.29 [s, 3 H phen *mer*(2H)/*fac*(1 H)], 8.61 (m, 1 H, phen *fac*), 8.90–9.00 (m, 2 H, phen *mer*), 9.21 (d, 1 H phen *fac*), 9.75 (d, 1 H phen *mer*), 9.95 (d, 1 H phen *mer*) ppm.

***mer*-[$RhCl_3$(dpq)(CH_3OH)]·$3H_2O$ (3):** Preparation as for **2** in CH_2Cl_2/MeOH (50 mL) with $RhCl_3·3H_2O$ (100.0 mg, 0.38 mmol) and dpq (88.2 mg, 0.38 mmol), suspended in CH_2Cl_2 (5 mL). Yield: 56.2% (107.5 mg) of a red solid. $C_{15}H_{12}Cl_3N_4O_1Rh·3H_2O$ (527.6): calcd. C 34.15, H 3.44, N 10.62; found C 33.9, H 3.0, N 11.0. LSIMS: *m*/*z* (%) = 437 (41) $[M – Cl]^+$, 405 (100) $[M – Cl – CH_3OH]^+$, 370 (55) $[M – Cl – HCl – CH_3OH]^+$. ^{1}H NMR (200 MHz, CD_3OD, 25 °C): δ = 3.78 (d, 3 H, CH_3, $MeOH_{coor}$), 8.19, 8.38 (2m, 2 H, dpq H3/8), 9.25 (s, 2 H, dpq H11/12), 9.70, 9.80 (2d, 2 H, dpq H4/7), 9.97, 10.16 (2d, 2 H, dpq H2/9) ppm.

[RhCl(bpy)(tpm)][PF_6]$_2$ (4): *mer*-[$RhCl_3$(DM*S*O)$_2$(DMS*O*)][39] (50.6 mg, 0.114 mmol) was stirred for 2 h at 70 °C with 2,2′-bipyridine (17.8 mg, 0.114 mmol) in MeOH/H_2O (1:1, 10 mL). Tris(pyrazolyl)methane (tpm) (24.4 mg, 0.114 mmol) was added and the solution was stirred for a further 2 h at 70 °C. Following solvent removal the resulting residue was redissolved in methanol. Addition of an excess of NH_4PF_6 led to precipitation of **4** as a colourless product. Yield: 41.2% (37.5 mg). $C_{20}H_{18}ClF_{12}N_8P_2Rh$ (798.7): calcd. C 30.08, H 2.27, N 14.03; found C 30.5, H 2.4, N 14.3. LSIMS: *m*/*z* (%) = 653 (12) $[M – PF_6]^+$, 507 (42) $[M – PF_6 – HPF_6]^+$. ^{1}H NMR (400 MHz, D_2O, 25 °C): δ = 6.54 (t, 1 H, tpm-22′), 6.92, (t, 2 H, tpm-22), 7.16 (d, 1 H tpm-23′), 7.87 (t, 2 H, bpy-4), 8.52 (t, 2 H, bpy-3), 8.54 (d, 2 H, tpm-23), 8.59 (d, 2 H, tpm-23′, tpm-21′), 8.67 (d, 2 H, tpm-21), 8.68 (d, 2 H, bpy-5), 8.81 (d, 2 H, bpy-2) ppm. UV/Vis (10 mM phosphate buffer, pH = 7.2, ε, $M^{-1}cm^{-1}$): λ_{max} = 308.5 (1.286×10^4), 317.5 (1.147×10^4) nm. Single crystals of **4** were obtained by slow evaporation of an aqueous solution.

[RhCl(bpm)(tpm)]Cl_2·$5H_2O$ (5): DMSO (26.8 μL) was added to a solution of $RhCl_3·3H_2O$ (100 mg, 0.38 mmol) in H_2O/MeOH (30 mL, 1:1) and the mixture was stirred for 1 h at 68 °C. 2,2′-Bipyrimidine (61.1 mg, 0.38 mmol) in 1:1 H_2O/CH_3OH (10 mL) was added and the mixture was stirred for a further 1 h at 68 °C. After addition of tpm (81.3 mg, 0.38 mmol) the solution was refluxed for 2 h. Following solvent removal the resulting residue was redissolved in methanol. Addition of diethyl ether led to precipitation of the yellow product, which was washed with CH_3OH and dried in vacuo. Yield: 44.3% (113.2 mg). $C_{18}H_{16}Cl_3N_{10}Rh·5H_2O$ (671.73): calcd. C 32.18, H 3.9, N 20.85; found C 31.9, H 3.8, N 20.8. LSIMS: *m*/*z* (%) = 545 (8) $[M – Cl]^+$, 509 (100) $[M – Cl – HCl]^+$. ^{1}H NMR (D_2O, 200 MHz, 25 °C): δ = 6.57 (t, 1 H, tpm-22′), 6.92 (t, 2 H, tpm-22), 7.36 (d, 1 H, tpm-23′), 8.11 (t, 2 H, bpm-3), 8.57–8.59 (m, 3 H, tpm-23, tpm-21′), 8.67 (d, 2 H, tpm-21), 9.05 (dd, 2 H, bpm-4), 9.51 (dd, 2 H, bpm-2) ppm.

[RhCl(phen)(tpm)][PF_6]$_2$·$2H_2O$ (6): Preparation as for **4** with 1,10-phenanthroline (20.5 mg, 0.114 mmol). Yield: 59.2% (55.5 mg). $C_{22}H_{18}ClF_{12}N_8P_2Rh·2H_2O$ (874.74): calcd. C 30.77, H 2.58, N 13.05; found C 30.5, H 2.5, N 13.4. LSIMS: *m*/*z* (%) = 677 (12) $[M – PF_6]^+$, 532 (47) $[M + H – 2PF_6]^+$, 497 (2) $[M + H – 2PF_6 – HCl]^+$. ^{1}H NMR (400 MHz, [D_6]DMSO, 25 °C): δ = 6.55 (t, 1 H, tpm-22′), 7.03 (t, 2 H, tpm-22), 7.29 (d, $^3J_{AB}$ = 6.3 Hz, 1 H, tpm-23′), 8.24 (t, 2 H, phen-3), 8.57 (s, 2 H, phen-5), 8.71 (d, $^3J_{AB}$ = 7 Hz, 1 H, tpm-21′) 8.76 (d, $^3J_{AB}$ = 6.3 Hz, 2 H, tpm-23), 8.83 (d, $^3J_{AB}$ = 7 Hz, 2 H, tpm-21), 9.03 (d, 2 H, phen-4), 9.21 (dd, $^3J_{AB}$ = 5.8, $^3J_{AC}$ = 6.3 Hz, 2 H, phen-2), 10.25 (s, 1 H, tpm-CH) ppm. Single crystals of [RhCl(phen)(tpm)][PF_6]$_2$·H_2O suitable for X-ray analysis were grown by slow evaporation of an aqueous solution.

[RhCl(tap)(tpm)]Cl_2·$2.5H_2O$ (7): Preparation as for **5** with tap (69.2 mg, 0.38 mmol). Yield: 57.9% (141 mg). $C_{20}H_{16}Cl_3N_{10}Rh·2.5H_2O$ (650.67): calcd. C 36.8, H 3.55 N 21.46; found C 37.1, H 3.1, N 21.2. LSIMS: *m*/*z* (%) = 569 (14) $[M – Cl]^+$, 533 (100) $[M – Cl – HCl]^+$. ^{1}H NMR (D_2O, 200 MHz, 25 °C): δ = 6.44 (t, 1 H, tpm-22′), 6.79 (d, $^3J_{AB}$ = 7 Hz, 1 H, tpm-23′), 6.99 (t, 2 H, tpm-22), 8.59 (d, $^3J_{AB}$ = 7.6 Hz 1 H, tpm-21′) 8.74 (2d, 4 H, tpm-23, tpm-21), 8.88 (s, 2 H, tap-5), 9.22 (d, $^3J_{AB}$ = 7.0 Hz 2 H, tap-3), 9.55 (d, $^3J_{AB}$ = 6.7 Hz, 2 H, tap-2) ppm.

[RhCl(dpq)(tpm)]Cl_2·$0.5H_2O$ (8): Tpm (36.5 mg, 0.17 mmol) dissolved in CH_3OH (10 mL) was added to a solution of [$RhCl_3$(dpq)(CH_3OH)]·$3H_2O$ **3** (80.9 mg, 0.17 mmol) in CH_3OH (10 mL) and refluxed for 2 h. Addition of diethyl ether led to precipitation of the product, which was washed with CH_3OH and dried in vacuo. Yield: 9.75% (64.8 mg). $C_{24}H_{18}Cl_3N_{10}Rh·0.5H_2O$ (664.74): calcd. C 43.36, H 2.88, N 21.07; found C 43.0, H 2.9, N 21.5. LSIMS: *m*/*z* (%) = 619 (46) $[M – Cl]^+$, 583 (57) $[M – Cl – HCl]^+$. 370 (100) $[M – Cl – HCl – tpm]^+$. ^{1}H NMR (CD_2Cl_2, 200 MHz, 25 °C): δ = 5.77 (t, 1 H, tpm-22′), 6.38 (t, 2 H, tpm-22), 7.59 (d, 2 H, tpm-23), 7.64 (d, 1 H, tpm-21), 8.22 (m, 2 H, dpq-3/8), 8.41 (d, 2 H, tpm-23′), 9.01 (d, 1 H, tpm-21′), 9.22 (d, 2 H, dpq-4/7), 9.29 (s, 2 H, dpq-11/12), 9.53 (d, 2 H, dpq-2/9) ppm.

[RhCl(dppz)(tpm)]Cl_2·$5H_2O$ (9): Preparation as for **5** with dppz (107.3 mg, 0.38 mmol) and CH_2Cl_2 instead of H_2O. Yield: 15.8% (47.5 mg). $C_{28}H_{20}Cl_3N_{10}Rh·5H_2O$ (795.87): calcd. C 42.26, H 3.8, N 17.6; found C 42.3, H 3.6, N 17.5. LSIMS: *m*/*z* (%) = 633 (20) $[M – Cl – HCl]^+$, 591 (100) $[M – Cl – CH]^+$. ^{1}H NMR (D_2O, 400 MHz, 25 °C): δ = 6.71 (t, 1 H, tpm-22′), 6.83 (t, 2 H, tpm-22), 7.01 (d, 1 H, tpm-23′), 7.88 (d, 2 H, dppz-11/14), 8.02 (m, 2 H, dppz-3/8), 8.27 (m, 2 H, dppz-12/13), 8.43 (d, 2 H, tpm-23), 8.53 (d, 1 H, tpm-21′), 8.74 (d, 2 H, tpm-21), 9.07 (d, 2 H, dppz-4/7), 9.71 (d, 2 H, dppz-2/9) ppm. UV/Vis (10 mM phosphate buffer, pH = 7.2, ε, $M^{-1}cm^{-1}$): λ_{max} = 278.5 (5.206×10^4) 362.5(1.229×10^4), 380.5(1.261×10^4) nm.

X-ray Structural Analysis of 4 and 6·H_2O: Crystal and refinement data for **4** and **6**·H_2O are summarised in Table 4. Intensity data for **4** and **6**·H_2O were collected on a an Oxford Diffraction Sapphire-CCD diffractometer at 108 K using 1° ω scans and Cu-K_α radiation (λ = 1.54178 Å). The data were corrected for absorption by the Gauss method for **4** and empirically for **6** and solved by direct methods with SHELX97. Refinement against F_o^2 was performed by SHELXL97[40] with anisotropic temperature factors for non-hydrogen atoms and protons at geometrically calculated positions as riding atoms. The relatively high R_1 and wR_2 values of 0.094 and

Table 4. Crystal and refinement data for complexes **4** and **6**.

	4	**6**
Empirical formula	$C_{20}H_{18}ClF_{12}N_8P_2Rh$	$C_{22}H_{18}ClF_{12}N_8OP_2Rh$
M [g/mol]	798.72	838.74
Temperature [K]	108	108
Crystal system	orthorhombic	monoclinic
Space group	$P2_12_12_1$	$P2_1/n$
a [Å]	7.6278(4)	11.675(2)
b [Å]	17.659(2)	12.3977(11)
c [Å]	20.047(1)	21.714(3)
α [°]	90	90
β [°]	90	98.908(14)
γ [°]	90	90
V [Å^3]	2699.9(3)	3105.0(8)
Z	4	4
F(000)	1576	1656
$D_{calcd.}$ [g/cm^3]	1.965	1.794
Crystal size [mm]	$0.554 \times 0.19 \times 0.136$	$0.382 \times 0.155 \times 0.062$
Radiation	Cu-K_α	Cu-K_α
μ [mm^{-1}]	8.218	7.208
θ_{max} [°]	64.13	65.1
h,k,l ranges	–8,8/–19,20/–23,22	–13,13/–12/13/–24,25
Collected reflections	11812	16634
Unique reflections	4182	4807
Observed reflections [$I > 2\sigma(I)$]	4027	3009
R_1 [$I > 2\sigma(I)$]	0.026	0.094
wR_2 (all data)	0.067	0.264
S [goodness-of-fit]	1.025	1.058
Max./min.$\Delta\rho$ [e Å^{-3}]	0.40/–0.80	2.51/–1.15
Flack parameter	0.072(7)	–

0.264, respectively, for compound **6** are due to dynamic disorder of the PF_6^- anion.

CCDC-725285 (for **4**) and -725286 (for **6**) contain the supplementary crystallographic data for this paper. These data can be obtained free of charge from The Cambridge Crystallographic Data Centre via www.ccdc.cam.ac.uk/data_request/cif.

DNA Binding Studies of 4–9: The UV/Vis kinetic studies and thermal denaturation temperature T_m determinations for 1:5 complex/DNA mixtures [DNA concentration = M(base pairs)] were performed in a 10 mM phosphate buffer at pH = 7.2. Melting curves were recorded at 2 °C steps for the wavelength 260 nm with an Analytik Jena SPECORD 200 spectrometer equipped with a Peltier temperature controller. ΔT_m values were calculated by determining the midpoints of melting curves from the first-order derivatives. The experimental ΔT_m values are estimated to be accurate within ±1 °C. Concentrations of CT DNA were determined spectrophotometrically using the molar extinction coefficient ε_{260} = 13200 M^{-1} cm^{-1}.[41]

Viscosity Measurements: Viscosities for complex/sonicated DNA mixtures were determined for **4** and **9** using a Cannon-Ubbelhode Semi-micro dilution viscosimeter (Series No 75, Cannon Instument Co) held at 25 °C. The viscosimeter contained 2 mL of 0.4 mM sonicated DNA solution in a phosphate buffer (10 mM, pH = 7.2). Complex solutions (0.2 mM) also containing sonicated DNA at the same concentration as in the viscosimeter (0.4 mM) were added in increments from 50 to 800 μL from a micropipet. Reduced viscosities η (η_0 reduced viscosity of the DNA solution in the absence of complex) were calculated by literature methods[32] and plotted as $(\eta/\eta_0)^{1/3}$ against r {r = [complex]/[DNA] where [DNA] is given in M (base pairs)}. Ethidium bromide was employed as a standard intercalator to confirm the experimental conditions in a separate determination.

Cell Cultures: MCF-7 breast cancer and HT-29 human colon carcinoma cells were maintained in 10% (v/v) fetal calf serum containing cell culture medium (minimum essential medium eagle supplemented with 2.2 g $NaHCO_3$, 110 mg/L sodium pyruvate and 50 mg/L gentamicin sulfate adjusted to pH 7.4) at 37 °C/ 5% CO_2 and passaged twice a week according to standard procedures.

Cytotoxicity Measurements: The antiproliferative effects of the compounds were determined following an established procedure.[42] In short, cells were suspended in cell culture medium (MCF-7: 10000 cells/mL, HT-29: 2850 cells/mL), and 100 μL aliquots thereof were plated in 96 well plates and incubated at 37 °C/ 5% CO_2 for 72 h (MCF-7) or 48 h (HT-29). Stock solutions of the compounds **3**–**9** in DMSO, **2** and **3** in DMF and **1** in H_2O were freshly prepared and diluted with cell culture medium to the desired concentrations (final DMSO concentration: 0.1% v/v). The medium in the plates was replaced with medium containing the compounds in graded concentrations (six replicates). After further incubation for 96 h (MCF-7) or 72 h (HT-29) the cell biomass was determined by crystal violet staining and the IC_{50} values were determined as those concentrations causing 50% inhibition of cell proliferation. Results were calculated from 2–3 independent experiments.

Cellular Uptake Studies: For cellular uptake studies, MCF-7 and HT-29 cells were grown until at least 70% confluency in 175 cm^2 cell culture flasks.[43] Stock solutions of complexes **1**–**9** in DMSO, DMF or H_2O were freshly prepared and diluted with cell culture medium to the desired concentrations (final DMSO concentrations: 0.1% v/v, final complex concentration: 10 μM). The cell culture medium of the cell culture flasks was replaced with 10 mL of the cell culture medium solutions containing **1**–**9** and the flasks were incubated for 6 h at 37 °C/5% CO_2. Afterwards the culture medium was removed, the cell layer washed with 10 mL PBS (phosphate buffered saline pH 7.4), treated with 2–3 mL trypsin solution

(0.05% trypsin, 0.02% EDTA in PBS) and incubated for 2 min at 37 °C/ 5% CO_2 after removal of the trypsin solution. Cells were resuspended in 10 mL PBS and cell pellets were isolated by centrifugation (room temperature, 2000 g, 5 min). The isolated cell pellets were resuspended in 1–5 mL twice distilled water. The rhodium content of the samples was determined by graphite furnace atom absorption spectrometry (GF-AAS) and the protein contents of seperate aliquots by the Bradford method. To correct for matrix effects in GF-AAS measurements, samples and standards were adjusted to the same protein concentration by dilution with twice-distilled water. Prior to GF-AAS analysis, 20 μL Triton X-100 (1%) and 20 μL nitric acid (13%) were added to each 200 μL sample of the cell suspension. Cellular uptake was expressed as ng rhodium per mg cell protein for data optained from 3 independent experiments.

Atomic Absorption Spectrometry: A Vario graphite-furnace atomic-absorption spectrometer (Analytik Jena) was employed for the Rh quantification using a wavelength of 343.5 nm with a bandpass of 0.5 nm. A deuterium lamp was employed for the background correction. Matrix containing standards were obtained by addition of rhodium stock solution (1 mg mL^{-1} Rh in 5% aqueous HCl) to untreated cell suspensions. Probes were injected at a volume of 20 μL into standard graphite tubes. Drying, pyrolysis and atomization were performed according to literature conditions.[19] During the temperature programme the graphite tube was purged with a constant argon flow, which was only halted during the zeroing and atomisation steps. Pyrolysis and atomisation temperatures were optimised prior to the experiments. The recovery rates of the metallodrugs were determined initially and used for calculation of the final experimental values. The mean integrated absorbances of duplicated injections were used thoughout the study. The characteristic concentration for the described method was 0.85 ± 0.05 (μg Rh L^{-1})/1% A.

Gel Electrophoresis: Samples were prepared in 10 mM TE buffer (10 mM Tris-HCl, 1 mM EDTA, pH 7.6) and contained 20 μM (bp) pBR322 double-stranded circular plasmid DNA (c = 4361 μmol L^{-1} in bp) and various concentrations of 2, 5 or 20 μM of the rhodium complexes **4** and **9**. Irradiation were carried out successively in 1.5 mL Eppendorf tubes using a 150 W Xenon lamp plus monochromator (Oriel). Samples (10 μL) were irradiated for 30 min or 1 h and stored at –20 °C. Controls without metal complexes were also tested in parallel for light damage. DNA single- and double-strand breaks were detected by gel electrophoresis assays using 1% agarose gels with 10 mM TAE (Tris-acetate-EDTA) as the running buffer (pH = 8.4). Gels were run in the dark for 45–75 min at 100 V and stained with aqueous ethidium bromide (0.5 μg/mL). They were documented by a Gel documentation station PEQLab BioVersion 3000 and quantified with Bio1D software.

Supporting Information (see also the footnote on the first page of this article): Figure S1 depicts CD spectra (230–400 nm) of CT DNA with complexes **5** or **7** at a [complex]/[DNA] ratio of 1:5, Figure S2 the UV/Vis spectra of complexes **4** and **9** in the range 230–350 and 230–400 nm, respectively. All spectra were recorded in a 10 mM phosphate buffer at pH = 7.2. Figure S3 depicts gel-retardation assays of plasmid pBR322 DNA after 1 h incubation with complex **4** or **9** in the dark and with irradiation at λ = 311 nm.

Acknowledgments

This work was funded by the Deutsche Forschungsgemeinschaft (DFG) within the research group FOR 630 "Biological Function of Organometallic Compounds". R. B. thanks the Ruhr-University Research School and the WASAG Foundation for the award of stipends. We are also grateful to Heike Scheffler and Manuela Winter for excellent technical support.

[1] K. E. Erkkila, D. T. Odom, J. K. Barton, *Chem. Rev.* **1999**, *99*, 2777–2795.
[2] C. Metcalfe, J. A. Thomas, *Chem. Soc. Rev.* **2003**, *32*, 215–224.
[3] N. J. Wheate, C. R. Brodie, J. G. Collins, S. Kemp, J. R. Aldrich-Wright, *Mini-Rev. Med. Chem.* **2007**, *7*, 627–648.
[4] B. M. Zeglis, V. C. Pierre, J. K. Barton, *Chem. Commun.* **2007**, 4565–4579.
[5] C. L. Kielkopf, K. E. Erkkila, B. P. Hudson, J. K. Barton, D. C. Rees, *Nat. Struct. Biol.* **2000**, *7*, 117–121.
[6] D. Herebian, W. S. Sheldrick, *J. Chem. Soc., Dalton Trans.* **2002**, 966–974.
[7] A. Frodl, D. Herebian, W. S. Sheldrick, *J. Chem. Soc., Dalton Trans.* **2002**, 3664–3673.
[8] S. Schäfer, I. Ott, R. Gust, W. S. Sheldrick, *Eur. J. Inorg. Chem.* **2007**, 3034–3046.
[9] E. L. Menon, R. Perera, M. Navarro, R. J. Kuhn, H. Morrison, *Inorg. Chem.* **2004**, *43*, 5373–5381.
[10] M. A. Jakupec, M. Galanski, V. B. Arion, C. G. Hartinger, B. K. Keppler, *Dalton Trans.* **2008**, 183–194.
[11] L. Ronconi, P. J. Sadler, *Coord. Chem. Rev.* **2007**, *251*, 1633–1648.
[12] P. J. Dyson, G. Sava, *Dalton Trans.* **2006**, 1929–1933.
[13] N. Katsaros, A. Anagnostopoulou, *Crit. Rev. Oncol. Hematol.* **2002**, *42*, 297–308.
[14] A. M. Angeles-Boza, H. T. Chifotides, J. D. Aquirre, A. Chouai, P. K. L. Fu, K. R. Dunbar, C. Turro, *J. Med. Chem.* **2006**, *49*, 6841–6847.
[15] P. Clu, H. He, X. Liu, *Prog. Chem.* **2006**, *18*, 1646–1651.
[16] M. Harlos, I. Ott, R. Gust, H. Alborzinia, S. Wölfl, A. Kromm, W. S. Sheldrick, *J. Med. Chem.* **2008**, *51*, 3924–3933.
[17] M. A. Scharwitz, I. Ott, R. Gust, A. Kromm, W. S. Sheldrick, *J. Inorg. Biochem.* **2008**, *102*, 1623–1630.
[18] M. Dobroschke, Y. Geldmacher, I. Ott, M. Harlos, L. Kater, L. Wagner, R. Gust, W. S. Sheldrick, A. Prokop, *ChemMedChem* **2009**, *4*, 177–187.
[19] M. A. Scharwitz, I. Ott, Y. Geldmacher, R. Gust, W. S. Sheldrick, *J. Organomet. Chem.* **2008**, *693*, 2299–2309.
[20] F. P. Pruchnik, P. Jakimowicz, Z. Ciunik, J. Zakrzewska-Czerwinska, A. Opolski, J. Wietrzyk, E. Wojdat, *Inorg. Chim. Acta* **2002**, *334*, 59–66.
[21] G. Mestroni, E. Alessio, A. Sessanti o Santi, S. Geremia, A. Bergamo, G. Sava, A. Boccarelli, A. Schettino, M. Coluccia, *Inorg. Chim. Acta* **1998**, *273*, 62–71.
[22] D. A. Medvetz, K. D. Stakleff, T. Schreiber, P. D. Custer, K. Hindi, M. J. Panzner, D. D. Blanco, M. J. Taschner, C. A. Tessier, W. J. Youngs, *J. Med. Chem.* **2007**, *50*, 1703–1706.
[23] R. Bieda, I. Ott, M. Dobroschke, A. Prokop, R. Gust, W. S. Sheldrick, *J. Inorg. Biochem.* **2009**, *103*, 698–708.
[24] K. Brandt, W. S. Sheldrick, *J. Chem. Soc., Dalton Trans.* **1996**, 1237–1243.
[25] P. Ballesteros, C. Lopez, C. Lopez, R. M. Claramunt, J. A. Jimenez, M. Cano, J. V. Heras, E. Pinilla, A. Monge, *Organometallics* **1994**, *13*, 289–297.
[26] C. J. Adams, N. G. Connelly, D. J. H. Emslie, O. D. Hayward, T. Manson, A. G. Orpen, P. H. Rieger, *Dalton Trans.* **2003**, 2835–2845.
[27] V. Gonzalez, H. Adams, J. A. Thomas, *Dalton Trans.* **2005**, 110–115.
[28] D. M. Gray, in: *Circular Dichroism and the Conformational Analysis of Biomolecules* (Ed.: G. D. Fasman), Plenum Press, New York, **1996**, p. 469–500.
[29] W. C. Johnson, in: *Circular Dichroism: Principles and Applications*, 2nd ed. (Eds.: N. Berova, K. Nakanishi, R. W. Woody), VCH Publishers, New York, **2000**, p. 523–540.
[30] S. Gençaslan, W. S. Sheldrick, *Eur. J. Inorg. Chem.* **2005**, 3840–3849.

[31] S. Schäfer, W. S. Sheldrick, *J. Organomet. Chem.* **2007**, *692*, 1300–1309.
[32] G. Cohen, H. Eisenberg, *Biopolymers* **1966**, *4*, 429–440.
[33] D. Suh, J. B. Chaires, *Bioorg. Med. Chem.* **1995**, *3*, 723–728.
[34] M. E. Hogan, N. Dattagupta, D. M. Crowthers, *Biochemistry* **1979**, *18*, 280–288.
[35] S. P. Foxon, C. Metcalfe, H. Adams, M. Webb, J. A. Thomas, *Inorg. Chem.* **2007**, *46*, 409–416.
[36] L. Dadci, H. Elias, U. Frey, A. Hörnig, U. Koelle, A. F. Merbach, H. Paulus, J. S. Schneider, *Inorg. Chem.* **1995**, *34*, 306–315.
[37] J. G. Collins, A. D. Sleemann, J. R. Alrich-Wright, I. Greguric, T. W. Hambley, *Inorg. Chem.* **1998**, *37*, 3133–3141.
[38] A. Delgadillo, P. Romo, A. M. Leiva, B. Loeb, *Helv. Chim. Acta* **2003**, *86*, 2110–2120.
[39] B. R. James, R. H. Morris, *Can. J. Chem.* **1980**, *58*, 399–408.
[40] G. M. Sheldrick, *SHELXS97* and *SHELXL97*, Göttingen, Germany, **1997**.
[41] H.-Q. Liu, T.-C. Cheung, S.-M. Peng, C.-M. Che, *J. Chem. Soc., Chem. Commun.* **1995**, 1787–1788.
[42] I. Ott, K. Schmidt, B. Kircher, P. Schumacher, T. Wiglenda, R. Gust, *J. Med. Chem.* **2005**, *48*, 622–629.
[43] I. Ott, H. Scheffler, R. Gust, *ChemMedChem* **2007**, *2*, 702–707.

Received: April 23, 2009
Published Online: July 23, 2009

